The 8th International Supercritical CO_2 Power Cycles Symposium
February 27 – 29, 2024, San Antonio, Texas
Paper #42

Comparative analysis of supercritical CO2 cycles

Krzysztof Badyda
Full Professor
Warsaw University of Technology
Warsaw, Poland

Arkadiusz Szczesniak
PhD
Warsaw University of Technology
Warsaw, Poland

Olaf Dybiński
PhD Candidate
Warsaw University of Technology
Warsaw, Poland

Piotr Lis
PhD
Warsaw University of Technology
Warsaw, Poland

Wladyslaw Kryllowicz
Full Professor
Warsaw University of Technology
Warsaw, Poland

Jarosław Milewski
Full Professor
Warsaw University of Technology
Warsaw, Poland

Prof. Jaroslaw Milewski works at the Warsaw University of Technology's Faculty of Power and Aeronautical Engineering, specifically in the Institute of Heat Engineering.

He serves as the Head of the Power Division at the Institute of Heat Engineering, Editor-in-Chief of the Journal of Power Technologies, and a Member of the Editorial Board of Applied Energy. Prof. Milewski also holds the position of Director of the Hydrogen and Fuel Cells Center at the Institute of Applied Research.

His expertise includes fuel cell research (Molten Carbonate Fuel Cells–MCFC and Solid Oxide Fuel Cells–SOFC) as well as other power sources, hybrid systems, advanced power systems (hydrogen-based), and steam/gas turbine power generation systems.

Prof. Milewski has considerable experience collaborating with the power engineering industry.

He has authored and co-authored over 300 publications and 5 or more patents, with a Hirsch index of 24 based on Google Scholar statistics. He teaches courses on turbomachinery, turbomachinery theory, environmental protection, numerical tools in power plant simulations, hybrid systems, and more.

ABSTRACT

The presents a simulation of three different configurations of super critical CO2 cycles: pre–compression, partial cooling, and recompression performed using commercially available software (Ebsilon). The highest thermal efficiency is obtained for the recompression cycle (35%).

All three cycles operate at 700°C. In addition to enjoying the highest efficiency, the recompression cycle involves a moderate number of elements - just one heat exchanger more than the simplest cycle (Pre-compression).

INTRODUCTION

Renewable power sources, e.g., solar power [1], are highly variable in terms of output in many parts of the world, hence their development should go hand-in-hand with measures to integrate them with energy systems, e.g., integration of solar power with CCS system [2]. A very promising approach for dealing with the variability of renewable resources is involvement of large-scale energy storage. There are several areas that still have development potential in this case: liquid or compressed air energy storage [3,4], heat storage [5] or power-to-gas-to-power [6]. The latter technology uses hydrogen produced from renewable energy in various electrolysis plants [7–13]. This hydrogen can then be co-fired by gas turbines [14,15] or used in fuel cells. Due to the high efficiency and environmental friendliness, high-temperature fuel cells seem to be very future-proof energy sources (in contrast to CHP systems based on internal combustion engines) [16], hence fuel cells such as SOFC [17–30] H+SOFC [31–33] and MCFC [34–41] should be considered as methods for energy recovery from hydrogen. Due to the fact that the MCFC operating temperature (around 650°C) fits the needs of the Brayton super CO_2 cycle, these two energy sources can be connected in series (S-CO2 as a bottoming cycle) to improve the efficiency of energy conversion [42].

Work on the properties of various working media for the supercritical cycle dates back to the 1960s [43]. CO_2 has proven to be the most appropriate operating medium for several reasons. One is that CO_2 has a lower critical point pressure than water and therefore allows it to operate at a lower pressure. Another argument is that the transport and thermodynamic properties are very well known for this working medium. CO_2 is readily available, cheap, and non-toxic. The thermodynamic cycle based on supercritical carbon dioxide has many advantageous features such as: high power in relation to the flow of the working medium, high efficiency (even 55% in ideal conditions), no cavitation and corrosion of the turbine blades. Almost 40 years later Dostal started researching supercritical carbon dioxide [44]. He dealt with the analysis of supercritical CO_2 systems for applications in nuclear power (for advanced nuclear reactors). He conducted an analysis of individual elements of the system as well as entire systems for this type of application. This was followed by a report that predicted the cost of supercritical CO_2 systems operating on the Brayton cycle for use in fourth generation nuclear reactors [45]. The two publications above gave rise to a series of other studies on supercritical carbon dioxide systems.

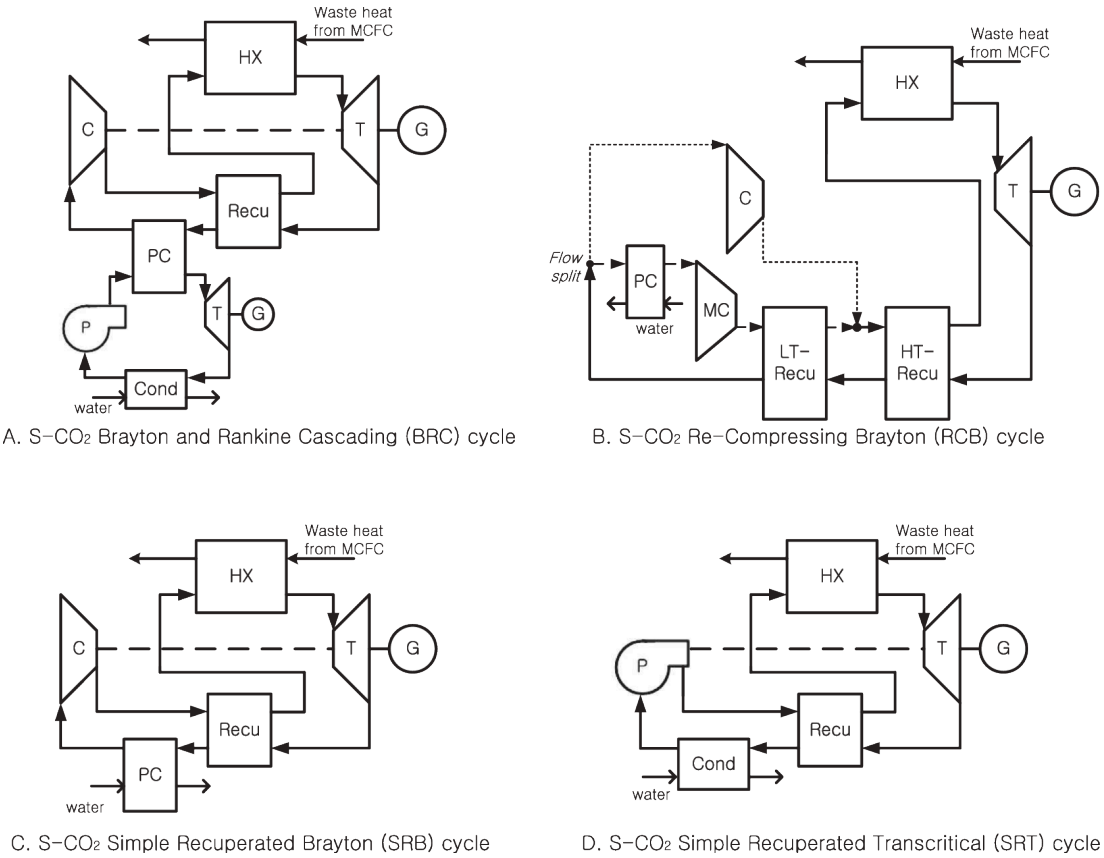

A. S-CO_2 Brayton and Rankine Cascading (BRC) cycle

B. S-CO_2 Re-Compressing Brayton (RCB) cycle

C. S-CO_2 Simple Recuperated Brayton (SRB) cycle

D. S-CO_2 Simple Recuperated Transcritical (SRT) cycle

Fig. 1 Various sCO_2 cycle layouts [42]

Different S-CO_2 cycles have been compared by Bae et al. (Fig. 1). As a result of this analysis, it was found that all cycles using super CO_2 in the Brayton cycle had better performance than the cycles using air as the working medium. The systems from Fig. 1 b, a and d contributed to the increase in the net efficiency of the entire hybrid system (MCFC - S-CO_2 system) by more than 10% in relation to the MCFC system without waste heat recovery [42]. The aim our paper is to develop models of the main elements of S-CO2 cycles as they are presented in Fig. 1. The following elements can be found in each system:

1. Compressor
2. Expander (turbine)
3. Heat Exchanger
4. Pump (in Rankine cycles)

Due to the relatively small sizes of the supercritical cycles, the turbomachinery used is also relatively small and often based on radial constructions (Fig. 6 and Fig. 11). The modeling of expanders and compressors is mainly based on energy balance equations, assuming constant efficiency; see [46]. More advanced studies like [47] take into consideration models which use mean-line flow analysis performance prediction for map of the off-design parameters. This approach involves four-dimensional parameter tables (rotational speed of the shaft, pressure, mass flow rate, and inlet temperature). To determine the output parameters (pressure and

temperature) the input parameters are interpolated. Generating four-dimensional maps takes a lot of work but works reasonably well. In fact, maps taken from this source were used in the present study.

For design purposes a detailed CFD can be used to model the CO_2 flow between turbomachinery blades, as shown in [48–50]; or more simply the similarity concept can be used [51]. Commercial software is available for estimating the main dimensions of the turbomachinery [52]. [53] shows a new method of modeling performance maps for stages of centrifugal compressor. Four dimensionless parameters were used to characterize the performance at the design point. Using this new approach, the entire performance map is based on these four parameters using algebraic equations that do not require exact knowledge of the geometry of the device.

A 1-d model for the design and evaluation of carbon dioxide compressor parameters is shown in [54]. A centrifugal compressor operating at high rotational speeds and mounted on foil gas bearings was modeled. The model was validated against data of Sandia Laboratories of a 50-kW compressor total efficiency.

Heat exchangers in S-CO_2 cycles operate at relatively low temperatures and high pressures. Serrano et al. [55] a methodology is presented which consists in designing heat exchangers in appropriate sizes for use in the Brayton cycle for supercritical CO_2. The working media on both sides of the heat exchanger (which cannot be too large) in such a cycle are characterized by a large pressure difference, therefore the use of PCHE (Printed Circuit Heat Exchangers) is suggested. Various empirical relationships between the Nusselt number and pressure drop were assessed there. The construction of a low-temperature regenerative heat exchanger and a pre-cooler were also tested using CFD methods due to the fact that they operate at near critical point of CO_2. In [56] the forced convection in a semicircular, printed circuit heat exchanger was modeled and experimentally validated for supercritical carbon dioxide as working medium and similar work was presented by [57]. For heat transfer in supercritical CO_2 during forced convection, a physically improved semi-empirical correlation with significantly improved predictions was proposed in [58].

RESULTS AND DISCUSSION

The most basic and compact supercritical CO_2 cycle is a simple Brayton cycle. It is simple and offers relatively good efficiency. However, there is still potential to improve its performance. The biggest reduction in efficiency of the supercritical Brayton cycle comes from the large irreversibility in the recuperator ([81]). Compound cycles have been introduced to overcome this problem and as shown later in this paper, these cycles perform significantly better than the regular supercritical Brayton cycle.

Pre-compression cycle

The pre-compression Brayton cycle is one of the ways to increase generation within the cycle and reduce the pinch point problem. As shown in Figure 11 the cycle is similar to the normal Brayton cycle with a small modification. First, the working fluid is compressed and then heated in the high temperature recuperator (1) using exhaust heat from the turbine. The fluid passes to a heat source (2), where heat is added, and then expands in the turbine (3). The remaining exhaust heat is extracted from the fluid in the high temperature recuperator (1). The difference from the normal Brayton cycle is that in the middle of the recuperation process, when the hot fluid temperature approaches the heated fluid temperature, a compressor (5) is introduced that compresses the fluid to a higher pressure. As the fluid pressure rises, so does its temperature

and specific heat. Thus, the regeneration process can continue, and more available heat is returned to the heated fluid. This extra heat reduces the average temperature at which heat is rejected from the cycle and increases the average temperature at which heat is added to the cycle. This results in an efficiency improvement of 6% over a Brayton cycle that would otherwise suffer from the pinch point problem ([84]).

Partial cooling cycle

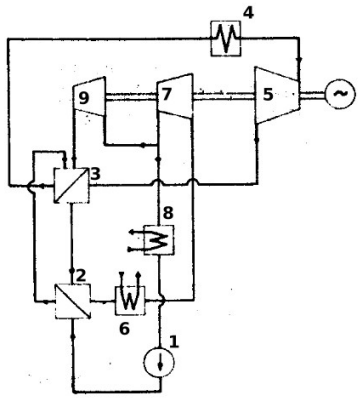

Figure 1 Layout of split-flow recompression Brayton cycle components ([81])

Another cycle layout that aims at reducing Brayton cycle drawbacks is the partial cooling cycle presented in Figure 10. In general, its operation differs from the previously described cycle in terms of two adjustments. The first is that only a fraction of the working fluid is compressed in the low temperature compressor (pump). The rest is compressed in the recompression compressor that is introduced before the pre-cooler and after the pre-compression compressor. The second difference is the introduction of another pre-cooler before the pre-compression compressor. This way, like the pre-compression cycle, more heat is available for the regeneration process.

After compression in the main compressor (1), a fraction of the working fluid is heated in the low temperature recuperator (2) and merged with the flow from the re-compressing compressors, which is at the same conditions. The fluid is then heated in the high temperature recuperator (3) and in the heat source (4) in turn and then enters the turbine (5). After the expansion process the fluid returns its heat in the high and low temperature recuperator (2,3). Then it passes to the pre-cooler (6) where it is cooled to the pre-compressor inlet temperature, and subsequently compressed in the pre-compressor (7). A part of the pre-compressed fluid is sent to the pre-cooler (8) and the main compressor. The rest is recompressed in the second recompressing compressor (9) to the high temperature recuperator inlet conditions, and then is merged with the stream from the main compressor. This move eliminates the pinch point problem, since due to the lower mass flow rate on the high-pressure side of the low temperature recuperator, the mass flow weighted heat capacity of the streams is about equal, and a pinch point does not occur.

The cycle improves its efficiency by reducing the average temperature of heat rejection so that the efficiency improvement is bigger than that for the pre-compression cycle.

Recompression cycle

Although the partial cooling cycle looks attractive due to its efficiency benefits, the complication

of the cycle layout may prove detrimental to the economic outcome. Therefore, another cycle is introduced, a recompression cycle, which is simpler than both the partial cooling and pre-compression cycle. The general layout of the cycle is shown in Figure 13.

The advantage of this cycle is that it eliminates one precooler and pre-compressing compressor from the cycle. After the regeneration process in the high temperature recuperator (3) the fluid is heated in the heat source (1) and passes to the turbine (2). Then it enters successively the high and low temperature recuperators (3,4) and returns its heat to the fluid on the high-pressure side. The fluid flow is then split into two streams. The first is sent directly to the recompression compressor, where it is compressed to the same pressure conditions as the CO_2 leaving the main compressor and merged with it in the high pressure recuperator. The second flow is cooled in the precooler (5), compressed in the main compressor (6) and heated in the recuperators.

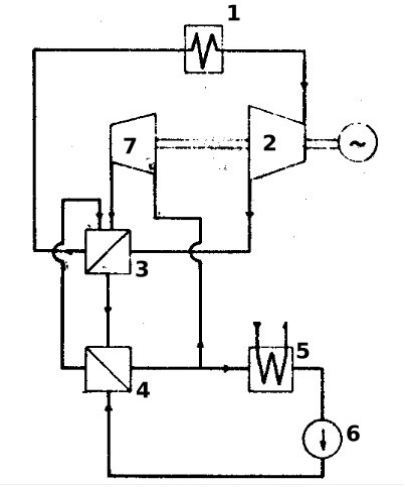

Figure 2 Schematic diagram of the recompression Brayton cycle ([81])

Table 1: Results comparison of various algorithms.

Parameter	Value
Turbine Inlet Temperature, °C	700
Turbine Inlet Pressure, MPa	20.2
Turbine Isentropic Efficiency, %	80
Compressor efficiency, %	85
Heat exchanger effectiveness	0.6

The effect of recompression is sufficient to overcome the pinch point problem. Owing to the decreased mass flow rate on the high-pressure side of the low temperature recuperator, the mass flow weighted heat capacity of the streams is about equal on both sides and a pinch point does not occur.

The recompression cycle is, along with the pre-compression cycle, the simplest among the surveyed cycles. In addition, at the desired operating conditions of turbine inlet pressures and temperatures (20 MPa and 550°C), it achieves the highest efficiency of all examined cycles ([81]). Therefore, the recompression cycle is usually selected as the best-suited cycle and investigated with respect to various applications in literature.

The main CO_2 cycles layouts presented here are simulated in EBSILON®Professional software to compare their performance based on the same mathematical model adopted in the simulation software. The CO_2 properties were simulated by means of “universal fluid” defined in the Refprop library, which is provided by EBSILON®Professional (version 12.01). The simulation of the most popular CO_2 layouts using the same simulation software and assumptions means a comprehensive comparison can be made of various CO_2 layouts, thereby eliminating the inaccuracies which are inevitable when using different models created by various authors.

Table 1 summarizes the input variables and constants which were used for the comparison of layouts.

The schematic diagram of the cycles implemented in EBSILON®Professional are shown in the following Figures: pre-compression Brayton cycle—Figure 12, partial cooling Brayton cycle—Figure 14, recompression Brayton cycle—Figure 16. The operating parameters for each layout are shown in Figure 13 (pre-compression cycle layout), Figure 15 (partial cooling cycle layout), Figure 17 (recompression cycle layout).

The simulation results revealed that the most efficient cycle layout is the recompression Brayton cycle—see Table 2. The displayed values in Table 2 corresponds to cycles operating with the assumptions given in Table 1.

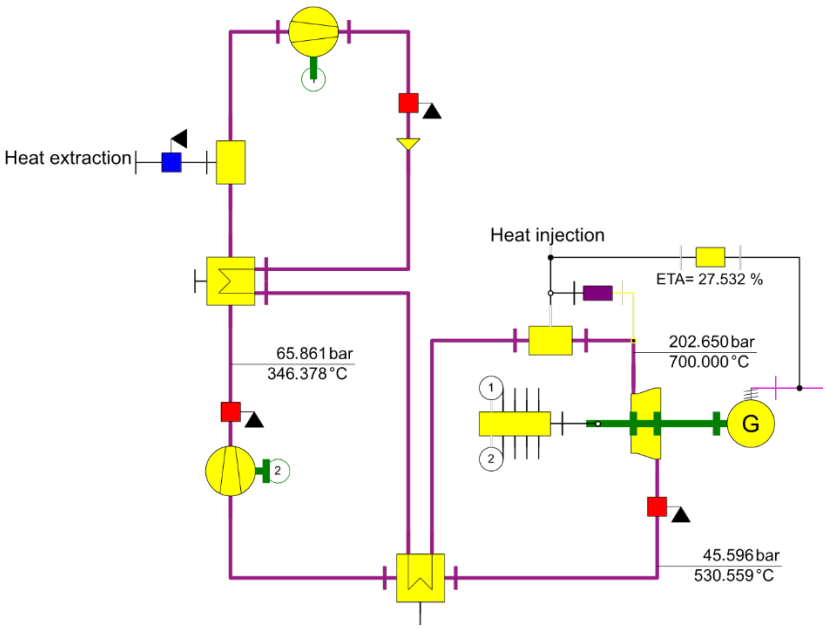

Figure 3 Schematic diagram of the pre-compression Brayton cycle implemented in Ebsilon software

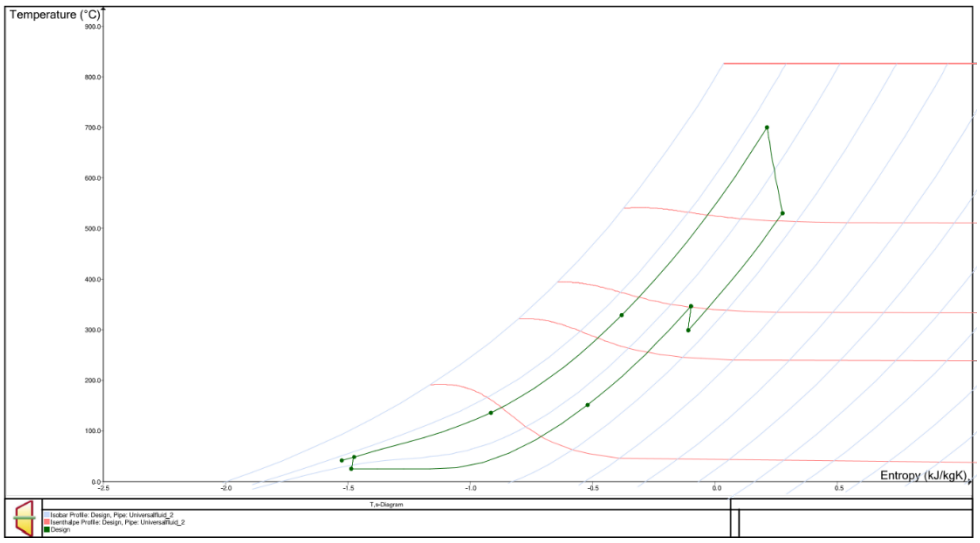

Figure 4 Temperature-entropy diagram of the pre-compression Brayton cycle implemented in Ebsilon software

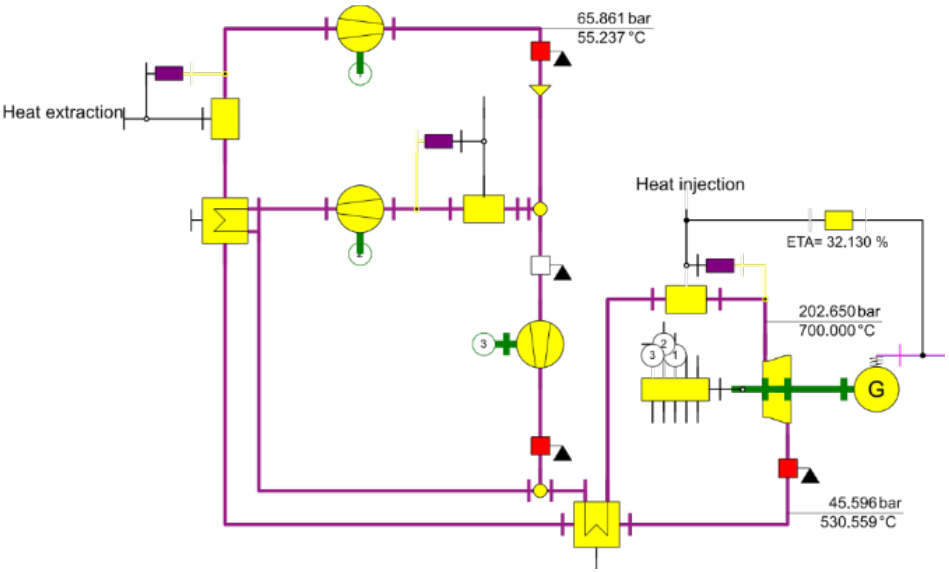

Figure 5 Schematic diagram of the partial cooling Brayton cycle implemented in Ebsilon software

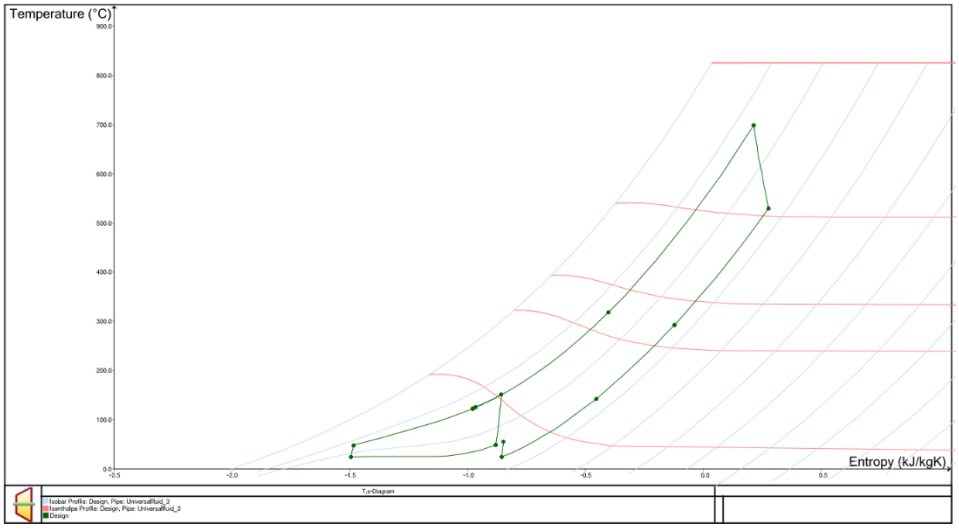

Figure 6 Temperature-entropy diagram of partial cooling Brayton cycle shown in T-s diagram

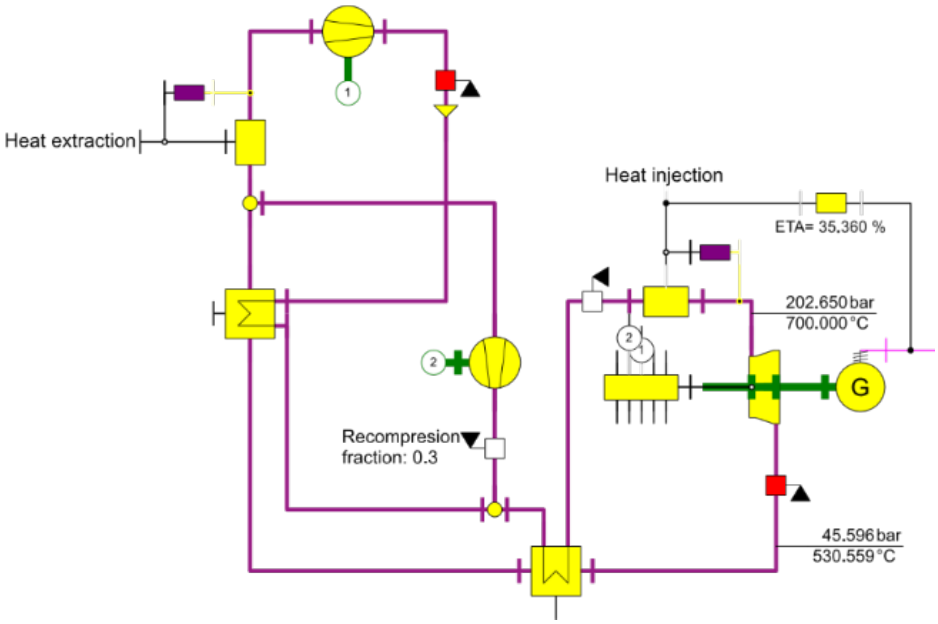

Figure 7 Schematic diagram of the recompression Brayton cycle implemented in Ebsilon software

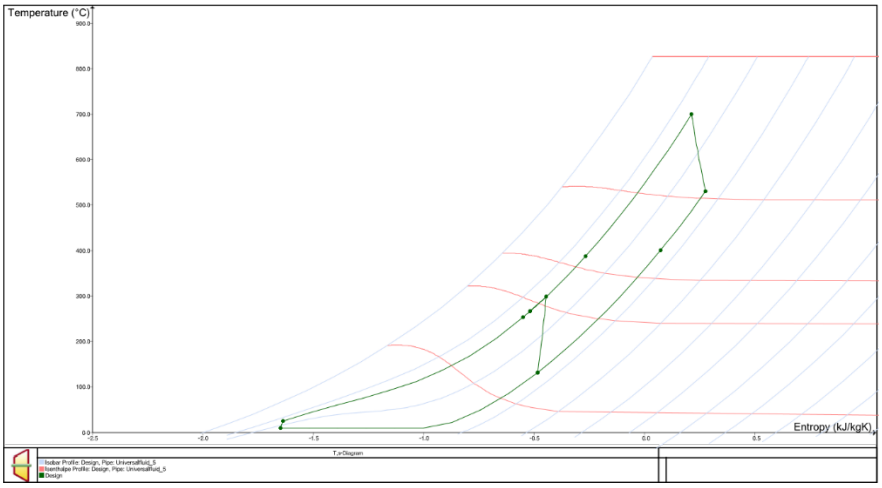

Figure 8 Temperature-entropy diagram of recompression Brayton cycle shown in T-s diagram

Table 2: Comparison of simulation results

Brayton cycle layout	Pre-compression	Partial cooling	Recompression
Cycle efficiency, %	27.5	32.1	35.4
Number of heat exchangers	2	1	2
Number of compressors	1	3	2
Number of expanders	1	1	1

The next step will be a detailed analysis of the Recompression Brayton cycle to identify its operational range in the off-design mode.

REFERENCES

[1] Siddiqui O, Dincer I. Analysis and performance assessment of a new solar-based multigeneration system integrated with ammonia fuel cell and solid oxide fuel cell-gas turbine combined cycle. J Power Sources 2017;370:138–54. https://doi.org/10.1016/j.jpowsour.2017.10.008.

[2] Bonaventura D, Chacartegui R, Valverde JM, Becerra JA, Ortiz C, Lizana J. Dry carbonate process for {CO} 2 capture and storage: Integration with solar thermal power. Renew & Sustain ENERGY Rev 2018;82:1796–812. https://doi.org/10.1016/j.rser.2017.06.061.

[3] Krawczyk P, Szabłowski Ł, Karellas S, Kakaras E, Badyda K. Comparative thermodynamic analysis of compressed air and liquid air energy storage systems. Energy 2018;142:46–54. https://doi.org/10.1016/j.energy.2017.07.078.

[4] Szablowski L, Krawczyk P, Badyda K, Karellas S, Kakaras E, Bujalski W. Energy and exergy analysis of adiabatic compressed air energy storage system. Energy 2017;138:12–8. https://doi.org/10.1016/j.energy.2017.07.055.

[5] MichałLeśko, Bujalski W. Modeling of District Heating Networks for the Purpose of Operational Optimization with Thermal Energy Storage. Arch Thermodyn 2017;38:139–63. https://doi.org/10.1515/aoter-2017-0029.

[6] Kotowicz J, Bartela L, Dubiel-Jurgas K. Analysis of energy storage system with distributed hydrogen production and gas turbine. Arch Thermodyn 2017;38:65–87. https://doi.org/10.1515/aoter-2017-0025.

[7] Clúa JGG, Mantz RJ, Battista H De. Optimal sizing of a grid-assisted wind-hydrogen system. Energy Convers Manag 2018;166:402–8. https://doi.org/10.1016/j.enconman.2018.04.047.

[8] Nadar A, Banerjee AM, Pai MR, Pai R V, Meena SS, Tewari R, et al. Catalytic properties of dispersed iron oxides Fe2O3/MO2 (M = Zr, Ce, Ti and Si) for sulfuric acid decomposition reaction: Role of support. Int J Hydrogen Energy 2018;43:37–52. https://doi.org/10.1016/j.ijhydene.2017.10.163.

[9] Senseni AZ, Meshkani F, Fattahi SMS, Rezaei M. A theoretical and experimental study of glycerol steam reforming over Rh/MgAl2O4 catalysts. ENERGY Convers Manag 2017;154:127–37. https://doi.org/10.1016/j.enconman.2017.10.033.

[10] Fukuzumi S, Lee Y-M, Nam W. Fuel Production from Seawater and Fuel Cells Using Seawater. ChemSusChem 2017;10:4264–76. https://doi.org/10.1002/cssc.201701381.

[11] Chen Y, Mojica F, Li G, Chuang P-YA. Experimental study and analytical modeling of an alkaline water electrolysis cell. Int J ENERGY Res 2017;41:2365–73. https://doi.org/10.1002/er.3806.

[12] Zhang C, Liu Q, Wu Q, Zheng Y, Zhou J, Tu Z, et al. Modelling of solid oxide electrolyser cell using extreme learning machine. Electrochim Acta 2017;251:137–44. https://doi.org/10.1016/j.electacta.2017.08.113.

[13] Olivier P, Bourasseau C, Bouamama PB. Low-temperature electrolysis system modelling: A review. Renew Sustain ENERGY Rev 2017;78:280–300. https://doi.org/10.1016/j.rser.2017.03.099.

[14] Mostowy M, Szablowski L. Comparison of the Brayton-Brayton Cycle with the Brayton-Diesel Cycle. J POWER Technol 2018;98:97–105.

[15] Zhuang Q, Geddis P, Runstedtler A, Bruce C, Clements B, Bruce C. An integrated natural gas power cycle using hydrogen and carbon fuel cells. FUEL 2017;209:76–84. https://doi.org/10.1016/j.fuel.2017.07.080.

[16] Carlucci AP, de Monte V, de Risi A, Strafella L. Benefits of Enabling Technologies for the ICE and Sharing Strategies in a CHP System for Residential Applications. J ENERGY Eng 2017;143. https://doi.org/10.1061/(ASCE)EY.1943-7897.0000434.

[17] Kupecki J, Motylinski K. Analysis of operation of a micro-cogenerator with two solid oxide fuel cells stacks for maintaining neutral water balance. Energy 2018;152:888–95. https://doi.org/10.1016/j.energy.2018.04.015.

[18] Prokop TA, Berent K, Iwai H, Szmyd JS, Brus G. A three-dimensional heterogeneity analysis of electrochemical energy conversion in {SOFC} anodes using electron nanotomography and mathematical modeling. Int J Hydrogen Energy 2018;43:10016–30. https://doi.org/10.1016/j.ijhydene.2018.04.023.

[19] Pianko-Oprych P, Hosseini SM. Dynamic Analysis of Load Operations of Two-Stage {SOFC} Stacks Power Generation System. ENERGIES 2017;10:2103. https://doi.org/10.3390/en10122103.

[20] Kupecki J, Motylinski K, Skrzypkiewicz M, Wierzbicki M, Naumovich Y. Preliminary electrochemical characterization of anode supported solid oxide cell (AS-SOC) produced in the Institute of Power Engineering operated in electrolysis mode (SOEC). Arch Thermodyn

2017;38:53–63. https://doi.org/10.1515/aoter-2017-0024.

[21] Zheng Y, Luo Y, Shi Y, Cai N. Dynamic Processes of Mode Switching in Reversible Solid Oxide Fuel Cells. J ENERGY Eng 2017;143. https://doi.org/10.1061/(ASCE)EY.1943-7897.0000482.

[22] Barelli L, Bidini G, Cinti G, Ottaviano A. Study of SOFC-SOE transition on a RSOFC stack. Int J Hydrogen Energy 2017;42:26037–47. https://doi.org/10.1016/j.ijhydene.2017.08.159.

[23] Genc O, Toros S, Timurkutluk B. Geometric optimization of an ejector for a 4~{kW} {SOFC} system with anode off-gas recycle. Int J Hydrogen Energy 2018;43:9413–22. https://doi.org/10.1016/j.ijhydene.2018.03.213.

[24] Azizi MA, Brouwer J. Progress in solid oxide fuel cell-gas turbine hybrid power systems: System design and analysis, transient operation, controls and optimization. Appl Energy 2018;215:237–89. https://doi.org/10.1016/j.apenergy.2018.01.098.

[25] Lorenzo G De, Fragiacomo P. Electrical and thermal analysis of an intermediate temperature {IIR}-{SOFC} system fed by biogas. Energy Sci {&} Eng 2018;6:60–72. https://doi.org/10.1002/ese3.187.

[26] Ferrel-Alvarez AC, Dominguez-Crespo MA, Cong H, Torres-Huerta AM, Brachetti-Sibaja SB, la Cruz W. Synthesis and surface characterization of the La0.7-xPrxCa0.3MnO3 (LPCM) perovskite by a non-conventional microwave irradiation method. J Alloys Compd 2018;735:1750–8. https://doi.org/10.1016/j.jallcom.2017.11.306.

[27] Abdalla AM, Hossain S, Azad AT, Petra PMI, Begum F, Eriksson SG, et al. Nanomaterials for solid oxide fuel cells: A review. Renew Sustain ENERGY Rev 2018;82:353–68. https://doi.org/10.1016/j.rser.2017.09.046.

[28] Peksen M. Safe heating-up of a full scale {SOFC} system using 3D multiphysics modelling optimisation. Int J Hydrogen Energy 2018;43:354–62. https://doi.org/10.1016/j.ijhydene.2017.11.026.

[29] Badur J, Lemanski M, Kowalczyk T, Pawel Z, Kornet S. VERIFICATION OF ZERO-DIMENSIONAL MODEL OF SOFC WITH INTERNAL FUEL REFORMING FOR COMPLEX HYBRID ENERGY CYCLES. Chem Process Eng Chem I Proces 2018;39:113–28. https://doi.org/10.24425/119103.

[30] Dillig M, Plankenbuehler T, Karl J. Thermal effects of planar high temperature heat pipes in solid oxide cell stacks operated with internal methane reforming. J Power Sources 2018;373:139–49. https://doi.org/10.1016/j.jpowsour.2017.11.007.

[31] Dzierzgowski K, Wachowski S, Gojtowska W, Lewandowska I, Jasinski P, Gazda M, et al. Praseodymium substituted lanthanum orthoniobate: Electrical and structural properties. Ceram Int 2018;44:8210–5. https://doi.org/10.1016/j.ceramint.2018.01.270.

[32] Danilov NA, Tarutin AP, Lyagaeva JG, Pikalova EY, Murashkina AA, Medvedev DA, et al. Affinity of {YBaCo} 4 O 7+$\updelta$ -based layered cobaltites with protonic conductors of cerate-zirconate family. Ceram Int 2017;43:15418–23.

https://doi.org/10.1016/j.ceramint.2017.08.083.

[33] Lyagaeva J, Vdovin G, Hakimova L, Medvedev D, Demin A, Tsiakaras P. BaCe0.5Zr0.3Y0.2-xYbxO3-delta proton-conducting electrolytes for intermediate-temperature solid oxide fuel cells. Electrochim Acta 2017;251:554–61. https://doi.org/10.1016/j.electacta.2017.08.149.

[34] Davoodi AH, Pishvaie MR. Plant-Wide Control of an Integrated Molten Carbonate Fuel Cell Plant. J Electrochem Energy Convers Storage 2018;15:21005. https://doi.org/10.1115/1.4039043.

[35] Chakravorty J, Sharma G, Bhatia V. Analysis of a DVR with Molten Carbonate Fuel Cell and Fuzzy Logic Control. Eng Technol Appl Sci Res 2018;8:2673–9.

[36] Jienkulsawad P, Saebea D, Patcharavorachot Y, Kheawhom S, Arpornwichanop A. Analysis of a solid oxide fuel cell and a molten carbonate fuel cell integrated system with different configurations. Int J Hydrogen Energy 2018;43:932–42. https://doi.org/10.1016/j.ijhydene.2017.10.168.

[37] Wu M, Zhang H, Liao T. Performance assessment of an integrated molten carbonate fuel cell-thermoelectric devices hybrid system for combined power and cooling purposes. Int J Hydrogen Energy 2017;42:30156–65. https://doi.org/10.1016/j.ijhydene.2017.10.114.

[38] Accardo G, Frattini D, Yoon SP, Ham HC, Nam SW. Performance and properties of anodes reinforced with metal oxide nanoparticles for molten carbonate fuel cells. J Power Sources 2017;370:52–60. https://doi.org/10.1016/j.jpowsour.2017.10.015.

[39] Cheon Y, Lee D, Lee I-B, Sung SW. A new {PID} auto-tuning strategy with operational optimization for {MCFC} systems. 2013 9th Asian Control Conf., IEEE; 2013. https://doi.org/10.1109/ascc.2013.6606304.

[40] Samanta S, Ghosh S. Techno-economic assessment of a repowering scheme for a coal fired power plant through upstream integration of SOFC and downstream integration of MCFC. Int J Greenh GAS Control 2017;64:234–45. https://doi.org/10.1016/j.ijggc.2017.07.020.

[41] Czelej K, Cwieka K, Colmenares JC, Kurzydlowski KJ. Atomistic insight into the electrode reaction mechanism of the cathode in molten carbonate fuel cells. J Mater Chem A 2017;5:13763–8. https://doi.org/10.1039/c7ta02011b.

[42] Bae SJ, Ahn Y, Lee J, Lee JI. Various supercritical carbon dioxide cycle layouts study for molten carbonate fuel cell application. J Power Sources 2014;270:608–18. https://doi.org/10.1016/j.jpowsour.2014.07.121.

[43] Feher EG. The supercritical thermodynamic power cycle. Energy Convers 1968;8:85–90. https://doi.org/http://dx.doi.org/10.1016/0013-7480(68)90105-8.

[44] Dostal V, Driscoll MJ, Hejzar P. A Supercritical Carbon Dioxide Cycle for Next Generation Nuclear Reactors. Adv Nucl Power Technol Progr 2004.

[45] Driscoll MJ. Supercritical CO2 Plant Cost Assessment 2004.

[46] Dostal V, Driscoll MJ, Hejzlar P. A supercritical carbon dioxide cycle for next generation nuclear reactors. Massachusetts Institute of Technology, Department of Nuclear Engineering, 2004.

[47] Pickard SAWRFRMEVGERPS. Operation and Analysis of a Supercritical CO2 Brayton Cycle. SANDIA Rep 2010.

[48] Pecnik Rene; Colonna P. Accurate CFD Analysis of a Radial Compressor Operating with Supercritical CO2. Supercrit. CO2 Power Cycle Symp., 2011.

[49] Schmitt J, Amos D, Custer C, Willis R, Kapat J. Study of A Supercritical CO2 Turbine with TIT fo 1350K for Brayton Cycle with 100MW class output: Aerodynamic analysis of Stage 1 Vane. 4th Int Symp - Supercrit CO2 Power Cycles 2014.

[50] Liu Z, Luo W, Zhao Q, Zhao W, Xu J. Preliminary Design and Model Assessment of a Supercritical {CO}2 Compressor. Appl Sci 2018;8:595. https://doi.org/10.3390/app8040595.

[51] Zhao Q, Mecheri M, Neveux T, Privat R, Jaubert J-N. Selection of a Proper Equation of State for the Modeling of a Supercritical CO2 Brayton Cycle: Consequences on the Process Design. Ind Eng Chem Res 2017;56:6841–53.

[52] Nassar A, Moroz L, Burlaka M, Pagur P, Govoruschenko Y. Designing Supercritical CO2 Power Plants using an Integrated System. Power-Gen India Cent Asia 201AD.

[53] Casey M, Robinson C. A Method to Estimate the Performance Map of a Centrifugal Compressor Stage. J Turbomach 2012;135:21034. https://doi.org/10.1115/1.4006590.

[54] Kus B, Nekså P. Development of one-dimensional model for initial design and evaluation of oil-free Co2 turbo-compressor. Int J Refrig 2013;36:2079–90. https://doi.org/10.1016/j.ijrefrig.2013.05.009.

[55] Serrano IP, Cantizano A, Linares JI, Moratilla BY. Modeling and sizing of the heat exchangers of a new supercritical {CO}2 Brayton power cycle for energy conversion for fusion reactors. Fusion Eng Des 2014;89:1905–8. https://doi.org/10.1016/j.fusengdes.2014.04.039.

[56] Li H, Zhang Y, Zhang L, Yao M, Kruizenga A, Anderson M. {PDF}-based modeling on the turbulent convection heat transfer of supercritical {CO} 2 in the printed circuit heat exchangers for the supercritical {CO} 2 Brayton cycle. Int J Heat Mass Transf 2016;98:204–18. https://doi.org/10.1016/j.ijheatmasstransfer.2016.03.001.

[57] Cui X, Guo J, Huai X, Cheng K, Zhang H, Xiang M. Numerical study on novel airfoil fins for printed circuit heat exchanger using supercritical {CO} 2. Int J Heat Mass Transf 2018;121:354–66. https://doi.org/10.1016/j.ijheatmasstransfer.2018.01.015.

[58] Meshram A, Jaiswal AK, Khivsara SD, Ortega JD, Ho C, Bapat R, et al. Modeling and analysis of a printed circuit heat exchanger for supercritical {CO} 2 power cycle applications. Appl Therm Eng 2016;109:861–70. https://doi.org/10.1016/j.applthermaleng.2016.05.033.

[59] Muzychka YS. Constructal multi-scale design of compact micro-tube heat sinks and heat exchangers. Int J Therm Sci 2007;46:245–52. https://doi.org/10.1016/j.ijthermalsci.2006.05.002.

[60] Bejan A. General criterion for rating heat-exchanger performance. Int J Heat Mass Transf 1978;21:655–8. https://doi.org/10.1016/0017-9310(78)90064-9.

[61] Iverson BD, Conboy TM, Pasch JJ, Kruizenga AM. Supercritical CO2 Brayton cycles for solar-thermal energy. Appl Energy 2013;111:957–70.

[62] Pasch J, Conboy T, Fleming D, Rochau G. Supercritical CO2 Recompression Brayton Cycle: Completed Assembly Description. SANDIA Rep 2012.

[63] Conboy T, Pasch J, Fleming D. Control of a Supercritical {CO}2Recompression Brayton Cycle Demonstration Loop. Vol. 8 Supercrit. {CO}2 Power Cycles$\mathsemicolon$ Wind Energy$\mathsemicolon$ Honor. Award., ASME; 2013. https://doi.org/10.1115/gt2013-94512.

[64] Milewski J, Badyda K, Miller A. Gas Turbines in Unconventional Applications. Effic. Perform. Robustness Gas Turbines, InTech; 2012. https://doi.org/10.5772/37321.

ACKNOWLEDGEMENTS

The research has been co-funded with the funds of NCBR (National Center of Research and Development), under UNICORN project, acquired based on decision no. TANGO-IVC/0010/2019-00.